Electronic Supplementary Material (ESI) for Sustainable Energy & Fuels.

From non-innocent to guilty: on the role of redox-active ligand in the electro-assisted reduction of CO_2 mediated by a cobalt(II)-polypyridyl complex

Supporting Information

N. Queyriaux,* K. Abel, J. Fize, J. Pécaut, M. Orio* and L. Hammarström*

Cyclic Voltammetry Measurements.

Cyclic voltammetry (CV) experiments were performed on an Autolab PGSTAT100 potentiostat controlled with GPES 4.9 software. Measurements were carried out in a three-electrode electrochemical cell using glassy carbon (GC) as the working electrode, a platinum wire as auxiliary electrode and a $Ag/AgNO_3$ reference electrode. All potentials given in this work are reported with respect to Fc^+/Fc couple, thanks to the addition of ferrocene as an internal standard after each experiment. The potential of the Fc^+/Fc couple was typically found at 0.035 V vs $Ag/AgNO_3$ in DMF. Unless otherwise stated, the solution concentrations were 1 mM for the cobalt complex and 0.1 M for the supporting electrolyte ($^nBu_4NPF_6$) in DMF. Prior measurements, the analysed solutions were gas-saturated using either Ar or CO_2.

Controlled-Potential Electrolysis.

Controlled-Potential Electrolysis (CPE) experiments were performed on a Bio-Logic SP300 potentiostat controlled with EC-LAB software. Measurements were carried out using a mercury pool cathode (active surface area of ~1.77 cm^2) and a Ag/AgCl reference electrode. A platinum electrode was placed in a separated compartment connected by a glass-frit. Prior to electrolysis, the electrolyte solutions were saturated with CO_2 by ~30 minutes bubbling. The electrochemical cell was then kept closed and gastight during the electrolysis. Typically, the volume of electrolyte working compartment was 8 mL and that in the counter compartment was 2 mL. Hydrogen produced during electrolysis was quantified with a PerkinElmer Clarus 500 gas chromatography equipped with a porapack Q 80/100 column (6′ × 1/8″) thermostated at 40 °C and a TCD detector thermostated at 100 °C. Carbon monoxide, methane, and other volatile hydrocarbons from the gas phase were analysed using a flame induction detector (FID). Formic acid concentrations were determined by ionic exchange chromatography (883 Basic IC, Metrohm).

Computational details

All theoretical calculations were performed with the ORCA program package.[1] Full geometry optimizations were carried out for all complexes using the GGA functional BP86[2-4] in combination with the TZV/P[5] basis set for all atoms and by taking advantage of the resolution of the identity (RI) approximation in the Split-RI-J variant[6] with the appropriate Coulomb fitting sets.[7] Increased integration grids (Grid4 in ORCA convention) and tight SCF convergence criteria were used. To ensure that the resulting structures converged to a local minimum on the potential energy surface, numerical frequency calculations were performed and resulted in only positive normal vibrations. Solvent effects were accounted for according to the experimental conditions. For that purpose, we used the DMF solvent (ε = 38.3) within the framework of the conductor like screening (COSMO) dielectric continuum approach.[8] The relative energies were computed from the gas-phase optimized structures as a sum of electronic energy, relativistic and thermal corrections to the free energy. Electronic structures were obtained from

single-point Broken-Symmetry DFT calculations using the hybrid functional B3LYP[9-10] together with the TZV/P basis set. All possible spin configurations for the broken-symmetry[11-13] calculations were generated with the "FlipSpin" feature of ORCA. Optical properties were predicted from additional single-point calculations using the hybrid functional CAM-B3LYP[14] together with the TZV/P[5] basis set. Electronic transition energies and dipole moments for all models were calculated using time-dependent DFT (TD-DFT)[15-17] within the Tamm-Dancoff approximation.[18,19] To increase computational efficiency, the RI approximation2[20] was used in calculating the Coulomb term. At least 40 excited states were calculated in each case and difference transition density plots were generated for each transition. For each transition, difference density plots were generated using the orca plot utility program and were visualized with the Chemcraft[21] program. The same procedure was also employed to generate and visualize spin density plots as well as molecular orbitals.

Chemical reductions

Chemical reduction experiments were performed using two different strategies relying either on decamethylcobaltocene $Co(Cp^*)_2$ (Method A), or potassium graphite KC_8 (Method B), as the reductants.

Method A. In an Ar-filled glovebox, a solution of **[1-Cl]**$^+$ (5.10^{-5} M in dry DMF) was prepared. 3 mL of this stock solution was introduced in a 1 cm optical pathlength screw cap UV-Vis cuvette. Evolution of the UV-Vis spectrum upon progressive addition of reductant solution aliquots ($1.5.10^{-3}$ M in dry DMF) was monitored using an Agilent 8353 diode array spectrometer equipped with optical fibers.

Method B. In an Ar-filled glovebox, a solution of **[1-Cl]**$^+$ (1.10^{-3} M in dry DMF) was prepared in a Fisher-Porter flask. Addition of the desired amount of reductant (1 or 2 equivalents) resulted in rapid color change. For CO_2 reactivity experiments, the Fisher-Porter flask was sealed, brought outside the glovebox and connected to a Schlenk line. Argon was removed under vacuum and the Fischer-Porter flask was refilled with CO_2 gas (1 bar). Finally, a 250 µL aliquot was collected and introduced in a 1 mm optical pathlength gas tight UV-Vis cuvette and a UV-Vis spectrum recorded using an Agilent 8353 diode array spectrometer.

Crystal Structure Analysis – X-ray crystallography

Diffraction data (Tables S23-S24) were collected using an Oxford Diffraction XCallibur S Kappa area detector four-circle diffractometer (Mo-Kα radiation $\lambda = 0.71073$ Å, graphite monochromator), controlled by the Oxford Diffraction CrysAlis CCD software. Unique intensities with $I > 10\sigma(I)$ detected on all frames using the Oxford Diffraction RED were used to refine the values of the cell parameters.

The substantial redundancy in data allows analytical absorption corrections to be applied using crystal shape determination for complex **1'**, and empirical absorption correction for complex **1**. The space group

was determined from systematic absences, and it was confirmed by the successful resolution of the structure. The structures were solved by charge flipping method using superflip software, in Olex1.2 environment. All the atoms were found by difference Fourier syntheses. All non-hydrogen atoms were anisotropically refined on F^2 using ShelXL program. Hydrogen atoms were fixed in ideal positions for complex $\mathbf{[2\text{-}Cl_2]^0}$ and found by fourier transformation and refined isotropically for complex $\mathbf{[1\text{-}Cl]^+}$. CCDC 1970565 ($\mathbf{[1\text{-}Cl]^+}$), CCDC 1970564 ($\mathbf{[2\text{-}Cl_2]^0}$) contain the supplementary crystallographic data for this paper. These data can be obtained free of charge from the Cambridge Crystallographic Data Center via www.ccdc.cam.ac.uk/datarequest/cif.

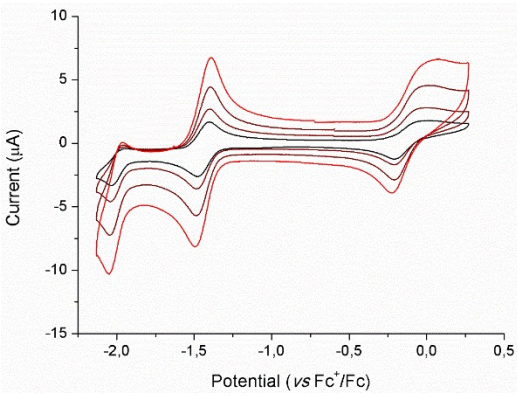

Figure S1. Cyclic voltammograms of complex **[1-Cl]**$^{+}$ in DMF solution (containing 0.1 M $^{n}Bu_4NBF_4$ as supporting electrolyte) at various scan rates (from black to red: 50, 100, 250 and 500 mV.s^{-1}). Working electrode: glassy carbon. Counter-electrode: Pt wire. Reference electrode: Ag/AgCl.

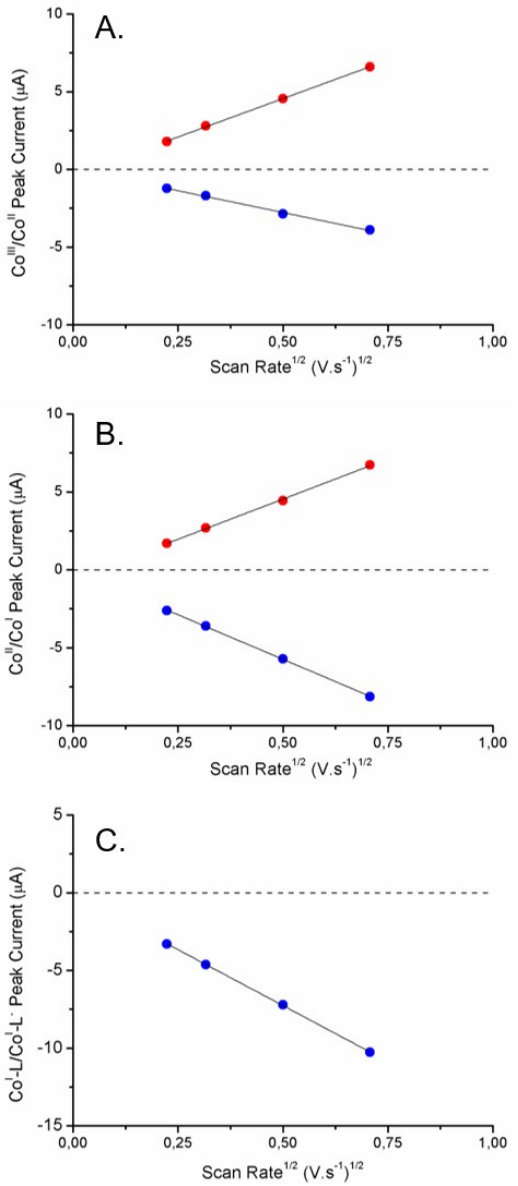

Figure S2. Linear plots of anodic and cathodic peak potential *versus* the square root of the scan rate of Co^{III}/Co^{II} (A), Co^{II}/Co^{I} (B) and Co^{I}-L/Co^{I}-$L^{\bullet -}$ (C) processes.

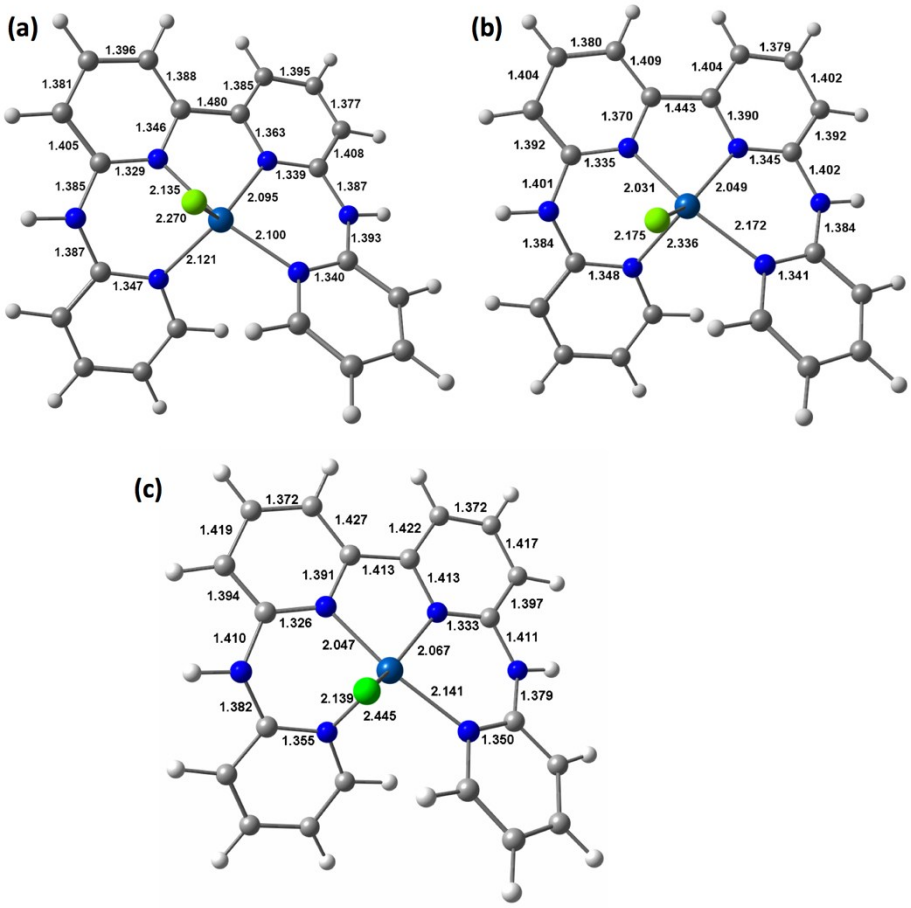

Figure S3. DFT-calculated geometries of (a) complex **[1-Cl]**$^{+}$ and (b) the one- and (c) two-electron reduced complexes **[1-Cl]**^{0} and **[1-Cl]**$^{-}$.

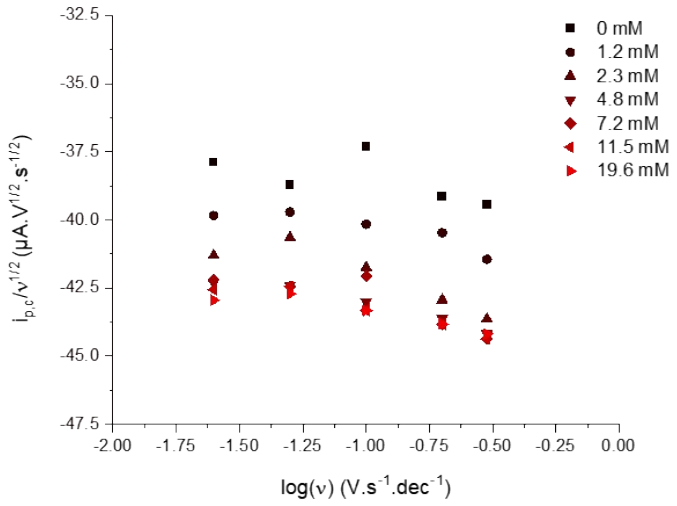

Figure S4. Evolution of the current function, $i_{p,c}/\nu^{1/2}$, recorded at different scan rates in the presence of increasing amounts of n-Bu_4NCl in DMF solution (containing 0.1 M $^{n}Bu_4NBF_4$ as supporting electrolyte). Working electrode: glassy carbon. Counter-electrode: Pt wire. Reference electrode: $Ag/AgNO_3$. Scan rate: 100 mV.s^{-1}.

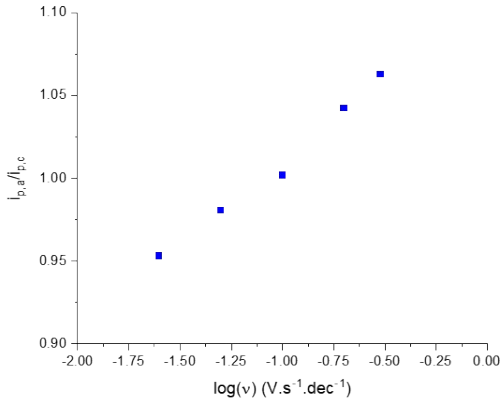

Figure S5. Ratio of anodic-to-cathodic currents for Co^{II}/Co^{I} couple recorded at different scan rates in DMF solution (containing 0.1 M $^{n}Bu_4NBF_4$ as supporting electrolyte). Working electrode: glassy carbon. Counter-electrode: Pt wire. Reference electrode: $Ag/AgNO_3$. Scan rate: 100 mV.s^{-1}.

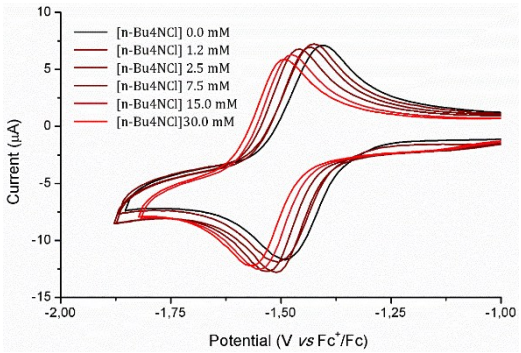

Figure S6. Selected cyclic voltammograms of complex **[1-Cl]**$^{+}$ in DMF solution (containing 0.1 M $^{n}Bu_4NBF_4$ as supporting electrolyte) in the presence of an increasing concentration of a chloride salt, n-Bu_4NCl. Working electrode: glassy carbon. Counter-electrode: Pt wire. Reference electrode: $Ag/AgNO_3$. Scan rate: 100 mV.s^{-1}.

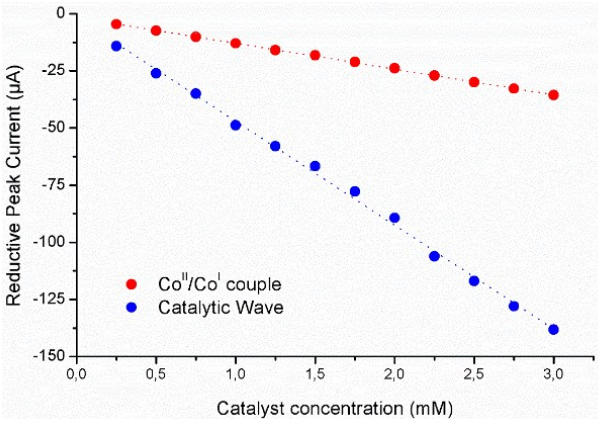

Figure S7. Plots of the cathodic peak currents associated with the Co^{II}/Co^{I} couple (red dots) or the catalytic wave (blue dots) *versus* the concentration of catalyst **[1-Cl]**$^{+}$ in solution. CVs recorded in CO_2-saturated DMF solutions (containing 0.1 M $^{n}Bu_4NBF_4$ as supporting electrolyte). Working electrode: glassy carbon. Counter-electrode: Pt wire. Reference electrode: $Ag/AgNO_3$. Scan rate: 100 $mV.s^{-1}$.

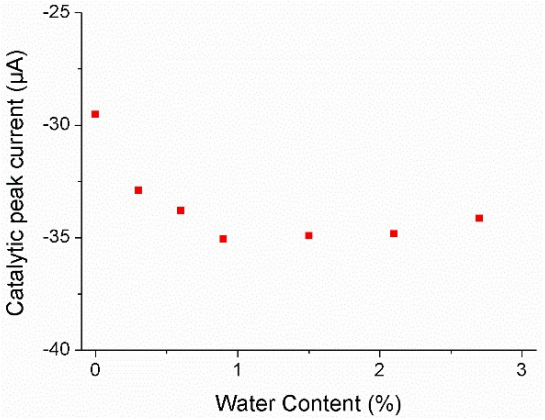

Figure S8. Plot of the catalytic peak currents *versus* the water content of the electrolyte solution. CVs were recorded in CO_2-saturated DMF solutions (containing 0.1 M $^{n}Bu_4NBF_4$ as supporting electrolyte). Working electrode: glassy carbon. Counter-electrode: Pt wire. Reference electrode: $Ag/AgNO_3$. Scan rate: 25 $mV.s^{-1}$.

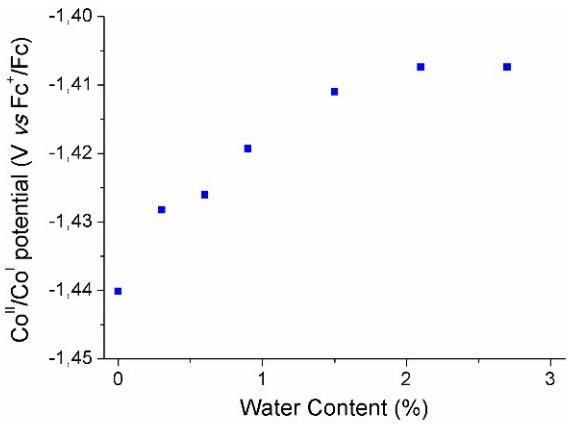

Figure S9. Plot of the evolution of the Co^{II}/Co^{I} potential *versus* the water content of the electrolyte solution. CVs were recorded in CO_2-saturated DMF solutions (containing 0.1 M $^{n}Bu_4NBF_4$ as supporting electrolyte). Working electrode: glassy carbon. Counter-electrode: Pt wire. Reference electrode: $Ag/AgNO_3$. Scan rate: 25 $mV.s^{-1}$.

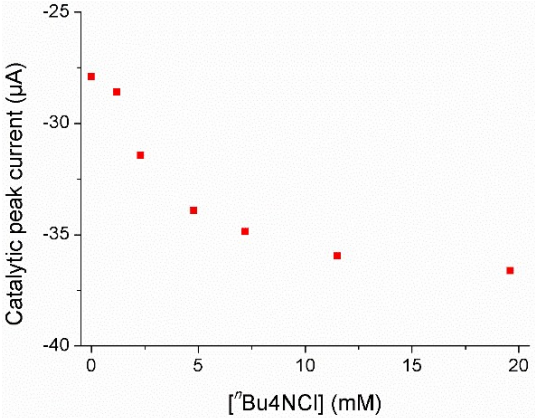

Figure S10. Plot of the catalytic peak currents *versus* the concentration of added $^{n}Bu_4NCl$ of the electrolyte solution. CVs were recorded in CO_2-saturated DMF solutions (containing 0.1 M $^{n}Bu_4NBF_4$ as supporting electrolyte). Working electrode: glassy carbon. Counter-electrode: Pt wire. Reference electrode: $Ag/AgNO_3$. Scan rate: 25 $mV.s^{-1}$.

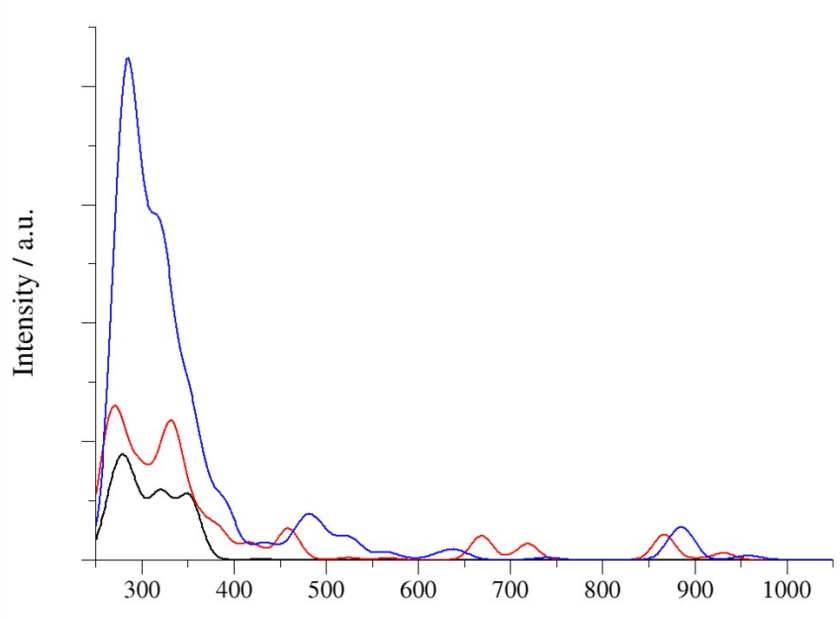

Figure S11. Theoretical fits of the UV-vis spectra of **[1-Cl]**$^{+}$ (black line), **[1-Cl]**^{0} (red line) and **[1]**^{0} (blue line).

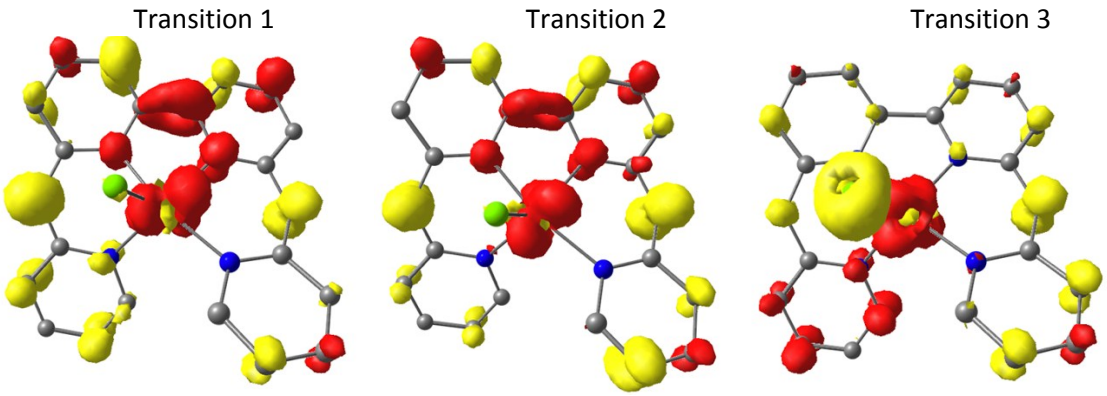

Figure S12. Difference electron densities sketch of transitions 1-3 for relevant transitions of **[1-Cl]**$^{+}$ (yellow = negative, red = positive density).

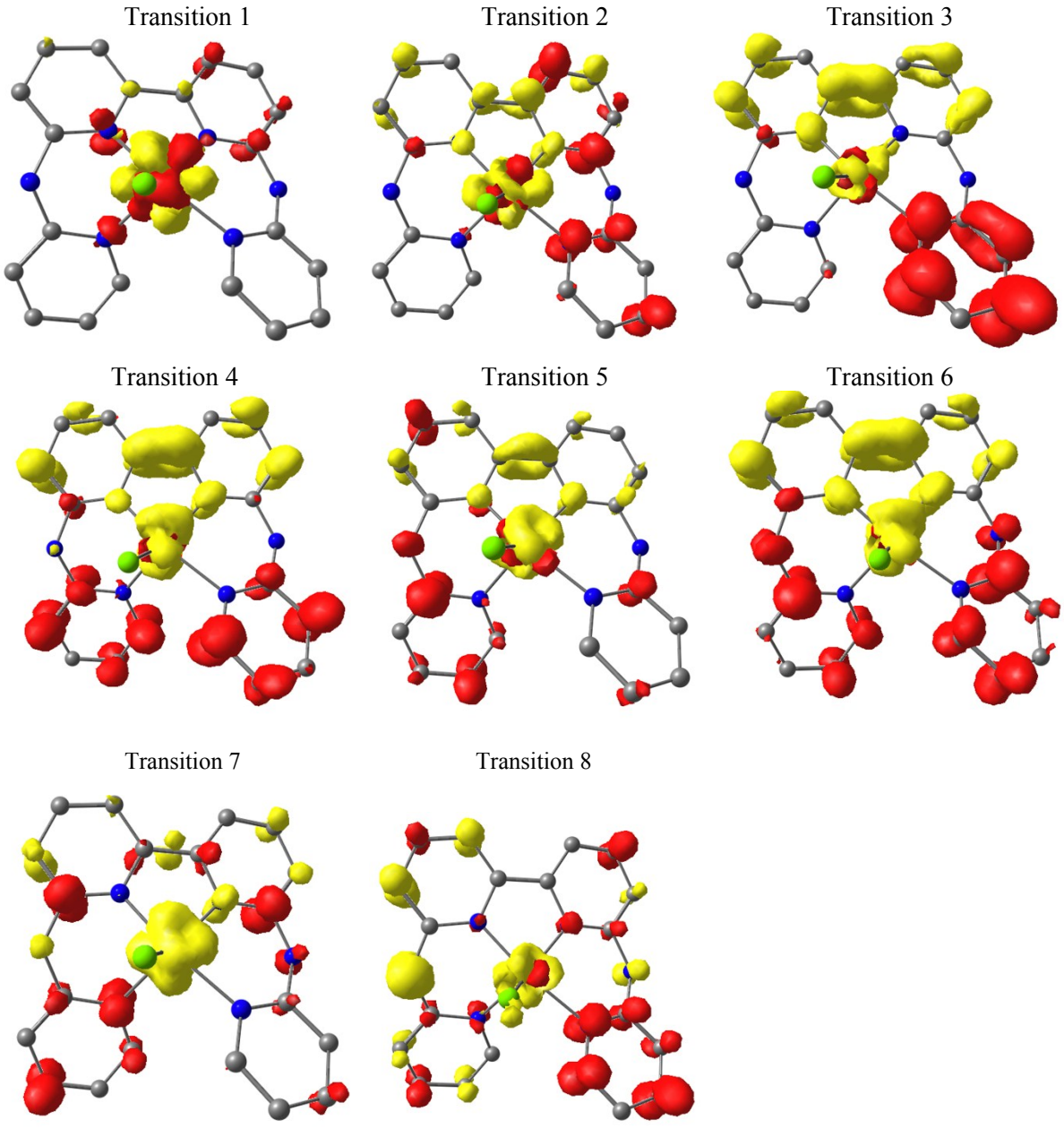

Figure S13. Difference electron densities sketch for relevant transitions of **[1-Cl]^0** (yellow = negative, red = positive density).

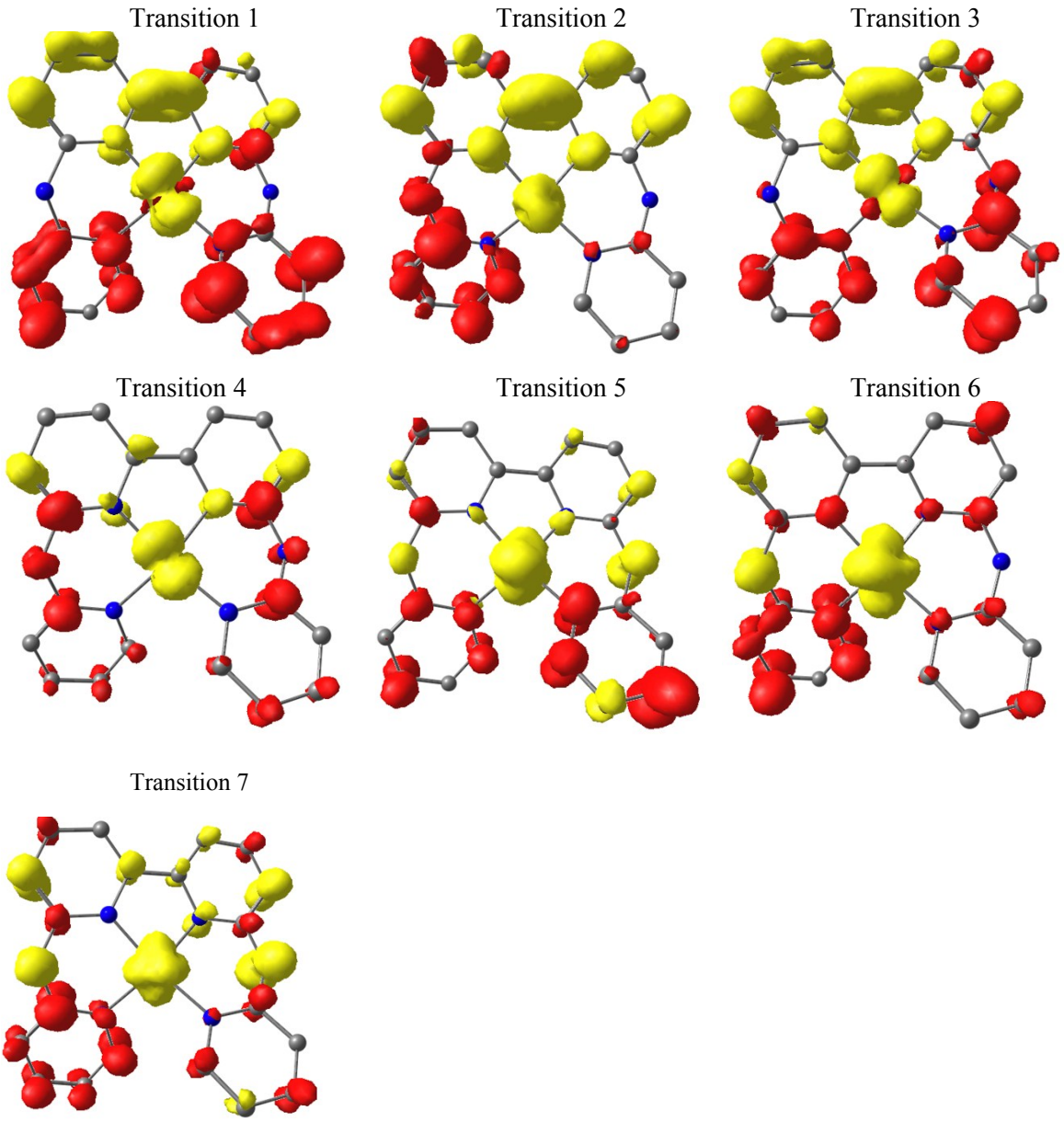

Figure S14. Difference electron densities sketch for relevant transitions of **[1]^0** (yellow = negative, red = positive density).

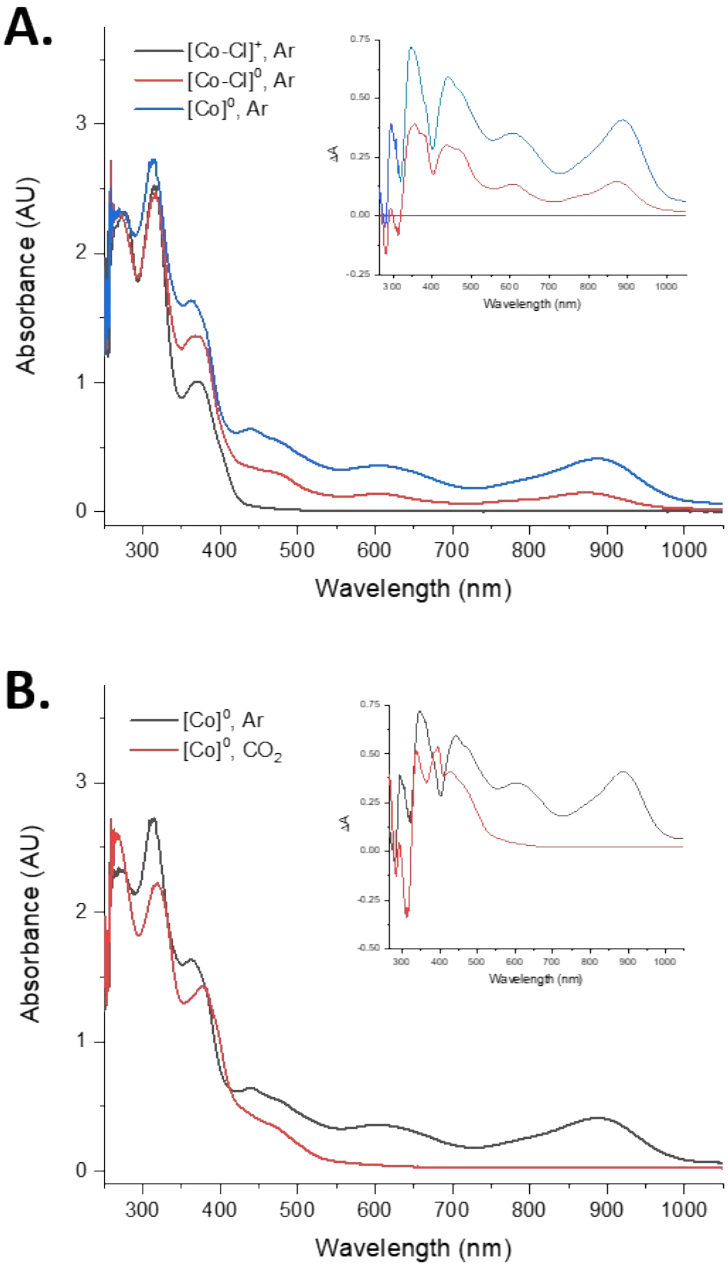

Figure S15. (**A**) Evolution of the UV-vis spectrum of **[1-Cl]**$^{+}$ in dry DMF in the absence of any added reductant in the medium (black trace) or in the presence of 1 equivalent (red trace) or 2 equivalents (blue trace) of potassium graphite. The insert displays differential spectra using unreduced **[1-Cl]**$^{+}$ spectrum as the reference. (**B**) UV-vis spectrum of the doubly reduced complex **[1]^{0}** in dry DMF recorded under argon (black trace) or under CO_2 (red trace). The insert displays differential spectra using unreduced **[1-Cl]**$^{+}$ spectrum as the reference.

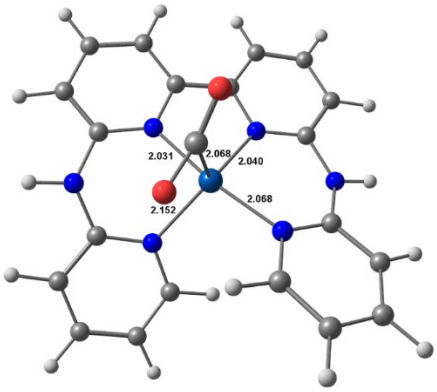

Figure S16. DFT-calculated geometries of the [**1**-(**C**OO)]^0 adduct.

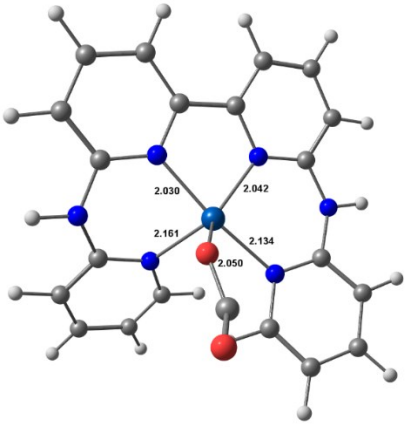

Figure S17. DFT-calculated geometries of the [**1**-(**O**CO)]^0 adduct.

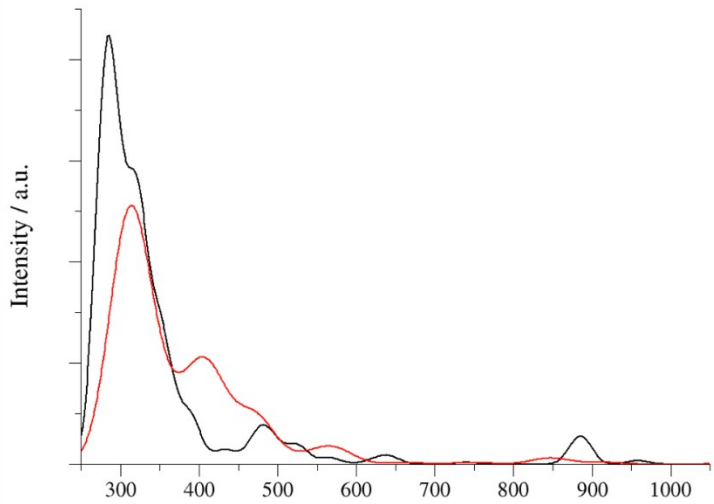

Figure S18. Theoretical fits of the UV-vis spectra of **[1-Cl]**$^-$ (black line) and **[1**-(**C**OO)]^0 (red line).

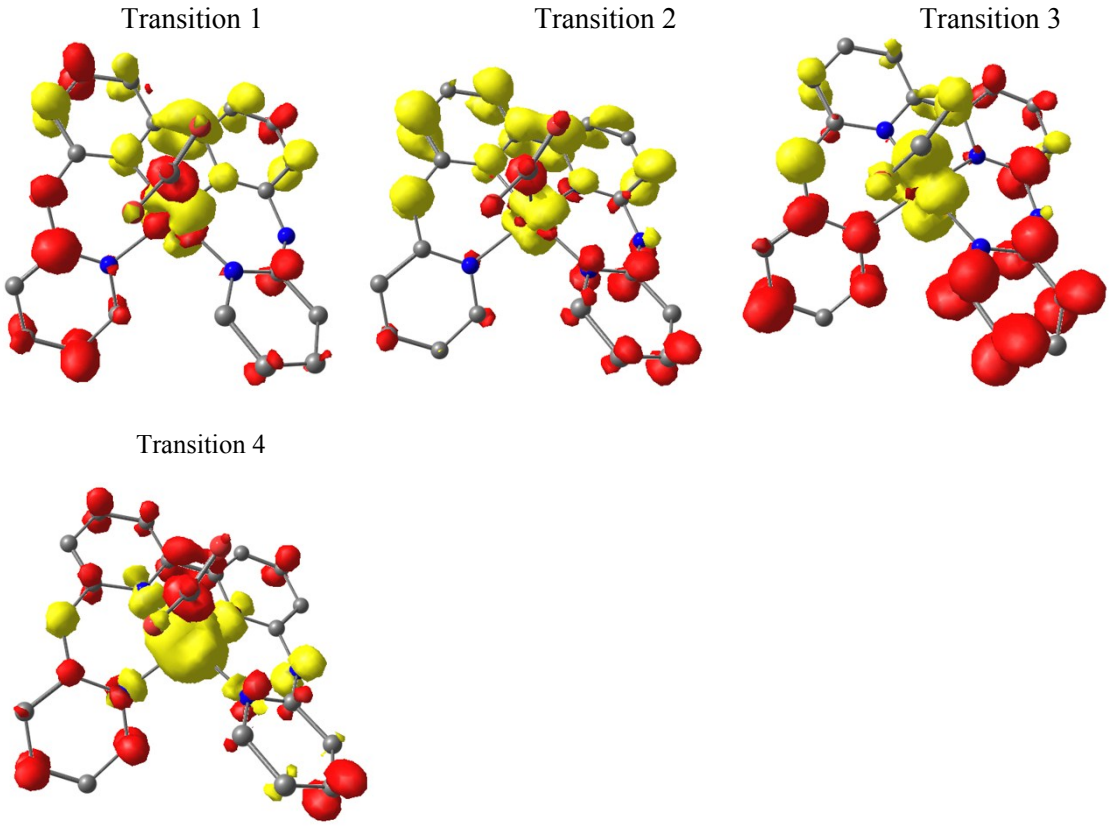

Figure S19. Difference electron densities sketch for relevant transitions of **[1-(**COO)**]**^{0}.

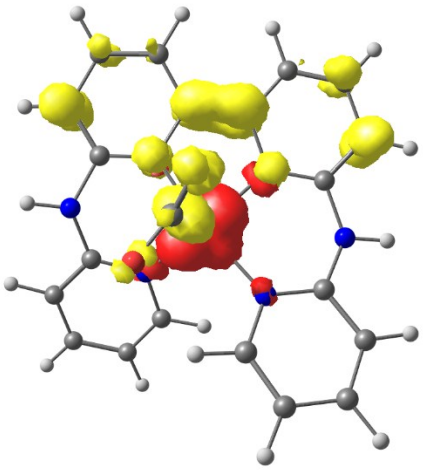

Figure S20. Spin density plot of the [**1**-(**C**OO)]^{0} adduct (Ms = ½).

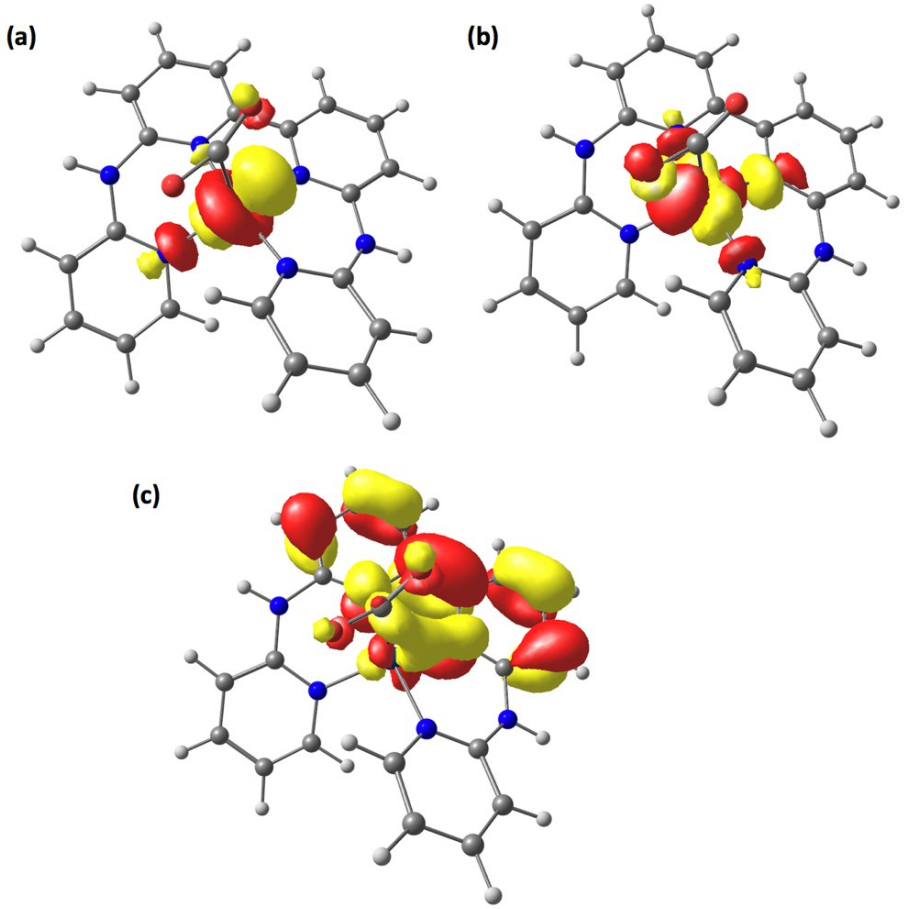

Figure S21. Unrestricted Corresponding Orbitals (UCOs) of the [**1**-(**C**OO)]^{0} adduct (Ms = ½).

Table S1. Selected bond lengths (Å) and angles (°) for the crystal structures of **[1-Cl]**$^{+}$ and **[2-Cl$_2$]**^{0}

Compounds	[Co(bapbpy)Cl]Cl (**[1-Cl]**$^{+}$)	[Co(bapbpy)Cl$_2$] (**[2-Cl$_2$]**^{0})
Selected bond lengths (in Å)		
Co – N1	2.094(3)	2.0747(12)
Co – N3	2.083(3)	2.0684(12)
Co – N4	2.063(3)	2.0691(12)
Co – N6	2.063(3)	2.0828(12)
Co – Cl1	2.3085(10)	2.5701(4)
Co – Cl2	Cl2 not coordinated	2.5499(4)
Selected angles (°)		
N1 – Co – Cl1	105.07(8)	84.03(3)
N3 – Co – Cl1	93.63(8)	99.08(3)
N4 – Co – Cl1	115.42(7)	83.41(3)
N6 – Co – Cl1	95.73(8)	92.81(4)
N1 – Co – Cl2	Cl2 not coordinated	90.76(3)
N3 – Co – Cl2	Cl2 not coordinated	84.75(3)
N4 – Co – Cl2	Cl2 not coordinated	102.64(3)
N6 – Co – Cl2	Cl2 not coordinated	84.69(4)
N4 – Co – N6	90.64(10)	89.68(5)
N3 – Co – N4	78.03(10)	79.20(5)
N1 – Co – N3	84.40(10)	88.33(5)
N6 – Co – N1	100.89(10)	105.60(5)

Table S2. Dihedral angles (°) α, β, γ, γ' as previously defined for a related copper(II) compound.

Compounds	[Co(bapbpy)Cl]Cl **[1-Cl]$^+$**	[Co(bapbpy)Cl_2] **[2-Cl_2]^0**
α	6.53	16.66
β	44.13	39.72
γ	19.13	22.69
γ'	23.47	21.27

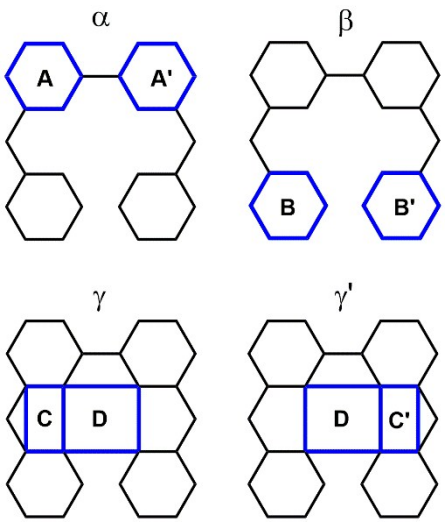

Table S3. Calculated Gibbs free energies for the spin states of **[1-Cl]$^+$**, the one- and two-electron reduced complexes **[1-Cl]^0** and **[1-Cl]$^-$**.

	Spin state	Gibbs free energy (Eh)	ΔG (kcal/mol)
[1-Cl]$^+$	S = 1/2	-2942.37344110	7.0
	S = 3/2	-2942.38468732	0
[1-Cl]^0	S = 1	-2941.71701610	0
	S = 2	-2941.70976548	4.5
[1-Cl]$^-$	S = 1/2	-2941.981944	20.5
	S = 3/2	-2942.014689	0

Table S4. Selected bonds length (Å) from DFT-calculated structures of **[1-Cl]**$^{+}$ and **[1-Cl]**^{0}.

Parameter	Co-N1	Co-N2	Co-N3	Co-N4	Co-Cl
[1-Cl]$^{+}$	2.135	2.095	2.121	2.100	2.270
[1-Cl]^{0}	2.031	2.049	2.175	2.172	2.336

Table S5. DFT-calculated relative stabilities of the reduced complexes under investigation.

System	Gibbs free energy (Eh)	ΔG (kcal/mol)
[1]$^{+}$ (S=1)	-2481.800140	-
Cl^{-}	-460.23455932	-
[1]$^{+}$ + Cl^{-}	-2942.034699	0
[1-Cl]^{0} (S =1)	-2942.033161	1.0

Table S6. Selected bonds length (Å) from DFT-calculated structures of **[1-Cl]**^{0} and **[1-Cl]**$^{-}$.

Parameter	Co-N1	Co-N2	Co-N3	Co-N4	N1-C1	C1-C2	C2-C3	C3-C4
[1-Cl]^{0}	2.031	2.049	2.175	2.172	1.370	1.409	1.380	1.404
[1-Cl]$^{-}$	2.047	2.067	2.139	2.141	1.391	1.427	1.372	1.419
Δ	+0.016	+0.018	-0.036	-0.031	+0.021	+0.018	-0.008	+0.015

Parameter	C4-C5	C5-N1	N2-C20	C20-C21	C21-C22	C22-C23	C23-C24	C24-N2
[1-Cl]^{0}	1.392	1.335	1.390	1.404	1.379	1.402	1.392	1.345
[1-Cl]$^{-}$	1.394	1.326	1.413	1.422	1.372	1.417	1.397	1.333
Δ	+0.002	−0.009	+0.023	+0.018	-0.007	+0.015	+0.005	-0.012

Table S7. DFT-calculated relative stabilities of the reduced complexes under investigation.

System	Gibbs free energy (Eh)	ΔG (kcal/mol)
[1]^{0} (S=3/2)	-2481.893546	-
Cl^{-}	-460.23455932	-
[1]^{0} + Cl^{-}	-2942.128105	0
[1-Cl]$^{-}$ (S =3/2)	-2942.111472	10.4

Table S8. DFT-calculated relative stabilities of **[1-Cl]**$^{+}$ and **[2-Cl$_2$]**^{0}.

System	Gibbs free energy (Eh)	ΔG (kcal/mol)
[1-Cl]$^{+}$ (S=3/2)	-2942.38468732	-
Cl^-	-460.23455932	-
[1-Cl]$^{+}$ + Cl^-	-3402.61924664	0
[2-Cl$_2$]^{0} (S =3/2)	-3402.61446579	3.0

Table S9. Calculated electronic transitions of **[1-Cl]**$^{+}$.

Transition	λ^{calc} **(nm)**	f^{calc} **(nm)**	**Assignment**
1	389	0.083	LMCT
2	353	0.057	LMCT
3	278	0.133	LMCT

Table S10. Calculated electronic transitions of **[1-Cl]**^{0}.

Transition	λ^{calc} **(nm)**	f^{calc} **(nm)**	**Assignment**
1	931	0.008	d-d
2	867	0.030	(ML)-(ML)CT
3	718	0.020	(ML)-LCT
4	669	0.029	(ML)-LCT
5	457	0.035	(ML)-LCT
6	419	0.017	(ML)-LCT
7	333	0.066	MLCT
8	259	0.058	MLCT

Table S11. Calculated electronic transitions of **[1]^0**.

Transition	λ^{calc} (nm)	f^{calc} (nm)	Assignment
1	889	0.025	(ML)-(ML)CT
2	647	0.012	(ML)-LCT
3	528	0.017	(ML)-LCT
4	475	0.048	MLCT
5	389	0.048	MLCT
6	320	0.140	MLCT
7	279	0.192	MLCT

Table S12. DFT-calculated relative stabilities of the CO_2-adducts under investigation.

System	Gibbs free energy (Eh)	**Δ**G (kcal/mol)
[**1**-(**C**OO)]^0	-2670.065093	0
[**1**-(**O**CO)]^0	-2670.032557	20.4

Table S13. Calculated electronic transitions of [**1**-(**C**OO)]^0.

Transition	λ^{calc} (nm)	f^{calc} (nm)	Assignment
1	575	0.027	(ML)-(ML)CT
2	465	0.059	(ML)-LCT
3	409	0.072	MLCT
4	306	0.137	MLCT

Table S14. DFT-calculated relative stabilities of the spin configurations of [**1**-(**C**OO)] ^{0}

System	Spin state	E (Eh)	Stability (cm^{-1})
[**1**- (**C**OO)]^0	Ms = 1/2	2670.385940	133
	S = 3/2	-2670.384661	0

Table S15. Cartesian coordinates for the DFT-optimized structure of **[Co^{II}(*bapbpy*)Cl]$^{+}$** (**[1-Cl]$^{+}$**)

27	-5.156443000	13.042835000	15.742671000
17	-7.184887000	13.700160000	16.521537000
7	-3.489698000	13.042744000	17.011649000
7	-4.485142000	15.068287000	15.674909000
7	-3.333271000	10.676769000	17.179849000
1	-2.760912000	9.953671000	17.593429000
7	-5.294392000	13.301198000	13.642051000
6	-3.029149000	14.274468000	17.368936000
7	-5.826235000	15.615417000	13.842904000
1	-6.315013000	16.367972000	13.379037000
6	-3.718327000	15.415405000	16.725683000
6	-1.333378000	13.292233000	18.741100000
1	-0.488318000	13.385903000	19.413662000
6	-4.764409000	8.799992000	16.813952000
1	-4.038408000	8.176812000	17.324900000
6	-2.899346000	11.951552000	17.514115000
6	-6.095168000	13.374291000	10.972726000
6	-1.797297000	12.045595000	18.385907000
1	-1.334939000	11.146829000	18.778333000
6	-1.954285000	14.431504000	18.227608000
1	-1.587852000	15.416677000	18.481552000
6	-5.756347000	14.445238000	13.101376000
7	-5.392145000	10.974898000	16.019817000
6	-6.184395000	14.500271000	11.762233000
1	-6.564941000	15.431648000	11.357477000
6	-4.521844000	10.176139000	16.653249000
6	-5.116176000	16.000249000	14.968492000
6	-5.188759000	12.216155000	12.841708000
1	-4.792634000	11.325800000	13.315944000
6	-6.872146000	9.103912000	15.718360000
1	-7.820460000	8.729857000	15.354409000
6	-6.559521000	10.439077000	15.588351000
1	-7.253825000	11.144190000	15.147446000
6	-5.940813000	8.263928000	16.334951000
1	-6.144375000	7.206054000	16.457658000
6	-5.564347000	12.201339000	11.516192000
1	-5.458188000	11.299165000	10.927466000
1	-6.418786000	13.408995000	9.938525000
6	-4.310443000	17.710171000	16.432427000
6	-3.609099000	16.734334000	17.143763000
6	-5.061136000	17.357170000	15.328378000
1	-4.260535000	18.747963000	16.741664000
1	-5.593673000	18.105056000	14.751700000
1	-3.021118000	17.006397000	18.009821000

Table S16. Cartesian coordinates for the DFT-optimized structure of **[Co^{II}(*bapbpy*)Cl_2]** (**[2-Cl_2]^0**)

27	11.423827000	7.306773000	2.246826000
17	13.281281000	8.820196000	2.850836000
17	9.501365000	6.079784000	1.301332000
7	12.294192000	7.111550000	0.261659000
7	12.786332000	5.803321000	2.874706000
7	8.670330000	8.097633000	3.956055000
7	14.274930000	6.059801000	1.046371000
7	10.162303000	9.073187000	2.385658000
7	10.580005000	6.698530000	4.100083000
6	13.536835000	6.674750000	0.043624000
6	9.009740000	9.102063000	3.059324000
6	13.972189000	5.575969000	2.306475000
6	9.360287000	7.039633000	4.520698000
6	14.149542000	6.789947000	-1.219333000
6	12.540114000	5.319937000	4.110980000
6	8.096712000	10.164748000	2.915459000
6	14.970979000	4.829373000	2.961093000
6	10.478167000	10.122757000	1.605299000
6	14.719815000	4.345317000	4.226547000
6	9.637513000	11.201003000	1.404711000
6	8.718524000	6.340212000	5.561038000
6	11.210115000	5.650740000	4.672337000
6	12.125968000	7.768606000	-2.041931000
6	11.597561000	7.613144000	-0.774667000
6	13.441848000	7.355801000	-2.259138000
6	8.409863000	11.208277000	2.069692000
6	13.485739000	4.592683000	4.823723000
6	10.630372000	4.905045000	5.691681000
6	9.361850000	5.267204000	6.138864000
1	15.227828000	5.872178000	0.772918000
1	11.136374000	4.043940000	6.106041000
1	13.282677000	4.252868000	5.830053000
1	7.735080000	8.196614000	4.321604000
1	7.729163000	6.639537000	5.889570000
1	8.877216000	4.703220000	6.928098000
1	7.165979000	10.161040000	3.473114000
1	10.568427000	7.865524000	-0.547650000
1	11.464847000	10.072936000	1.159471000
1	7.714737000	12.031462000	1.943733000
1	9.937164000	12.013150000	0.754428000
1	15.161012000	6.426384000	-1.368194000
1	11.523589000	8.190449000	-2.836722000
1	13.901310000	7.456020000	-3.236683000
1	15.923888000	4.650799000	2.474642000
1	15.482893000	3.785321000	4.755829000

Table S17. Cartesian coordinates for the DFT-optimized structure of **[Co^{I}(*bapbpy*)Cl]** (**[1-Cl]^{0}**)

27	-5.224380000	13.169419000	15.903133000
17	-7.466050000	13.465708000	16.488698000
7	-3.531562000	13.072680000	17.053968000
7	-4.569320000	15.088072000	15.785252000
7	-3.330842000	10.706196000	17.175804000
1	-2.750244000	9.986001000	17.580359000
7	-5.344490000	13.285970000	13.734904000
6	-3.078057000	14.325139000	17.450293000
7	-5.894650000	15.592863000	13.920987000
1	-6.356011000	16.348275000	13.435422000
6	-3.674212000	15.442707000	16.759560000
6	-1.493927000	13.326325000	18.964053000
1	-0.710929000	13.409964000	19.709502000
6	-4.632598000	8.795668000	16.586787000
1	-3.862827000	8.166546000	17.022847000
6	-2.949231000	11.988066000	17.596060000
6	-6.280417000	13.297190000	11.105314000
6	-1.933890000	12.062668000	18.545079000
1	-1.501103000	11.156905000	18.956492000
6	-2.065652000	14.454595000	18.414712000
1	-1.726096000	15.438070000	18.714353000
6	-5.850174000	14.413791000	13.198186000
7	-5.398590000	11.008587000	16.044406000
6	-6.349837000	14.436432000	11.879173000
1	-6.768795000	15.354406000	11.479685000
6	-4.476968000	10.199814000	16.587696000
6	-5.086602000	16.020343000	14.982631000
6	-5.253830000	12.196160000	12.948084000
1	-4.813908000	11.324859000	13.419507000
6	-6.754559000	9.088902000	15.518854000
1	-7.677926000	8.702227000	15.105248000
6	-6.523112000	10.450209000	15.547811000
1	-7.259018000	11.163672000	15.193781000
6	-5.771527000	8.243329000	16.041402000
1	-5.905193000	7.166340000	16.039596000
6	-5.696753000	12.145982000	11.640736000
1	-5.601924000	11.233699000	11.064459000
1	-6.659357000	13.306882000	10.088620000
6	-4.002521000	17.762593000	16.215014000
6	-3.398551000	16.803148000	17.001975000
6	-4.845649000	17.379917000	15.159586000
1	-3.808544000	18.814937000	16.393112000
1	-5.284260000	18.116054000	14.495002000
1	-2.728489000	17.097010000	17.799778000

Table S18. Cartesian coordinates for the DFT-optimized structure of **[Co^{I}(*bapbpy*)]$^{+}$** (**[1]**$^{+}$)

27	-4.791932000	13.002688000	15.603819000
7	-3.345655000	13.024737000	17.016355000
7	-4.542120000	14.975445000	15.772749000
7	-3.278623000	10.678077000	17.264910000
1	-2.776305000	9.939430000	17.738199000
7	-5.277826000	13.258217000	13.569256000
6	-2.976998000	14.271552000	17.432171000
7	-5.979315000	15.496664000	13.975470000
1	-6.480019000	16.262895000	13.546402000
6	-3.646389000	15.374057000	16.725192000
6	-1.443990000	13.317542000	19.009486000
1	-0.690812000	13.428891000	19.781350000
6	-4.758928000	8.861075000	16.828839000
1	-4.097634000	8.226449000	17.409876000
6	-2.834144000	11.946656000	17.623352000
6	-6.361223000	13.397776000	11.003163000
6	-1.849481000	12.054266000	18.616131000
1	-1.431230000	11.166145000	19.077569000
6	-2.025185000	14.444103000	18.429765000
1	-1.731002000	15.432630000	18.756424000
6	-5.885325000	14.382032000	13.146586000
7	-5.239229000	11.046759000	15.939080000
6	-6.456638000	14.471808000	11.862545000
1	-6.946797000	15.388389000	11.551172000
6	-4.447278000	10.225774000	16.661554000
6	-5.141819000	15.909196000	15.016758000
6	-5.172980000	12.225880000	12.700351000
1	-4.649159000	11.355778000	13.079545000
6	-6.750023000	9.203285000	15.546585000
1	-7.670546000	8.849085000	15.099542000
6	-6.379192000	10.520760000	15.415901000
1	-6.996907000	11.219165000	14.863075000
6	-5.906609000	8.348315000	16.267737000
1	-6.155875000	7.301058000	16.397703000
6	-5.688368000	12.245261000	11.422135000
1	-5.573787000	11.386367000	10.772608000
1	-6.789158000	13.458652000	10.008391000
6	-4.109458000	17.680392000	16.256848000
6	-3.420037000	16.721574000	16.990442000
6	-4.970016000	17.276698000	15.245239000
1	-3.957000000	18.735534000	16.452708000
1	-5.483630000	18.005412000	14.627300000
1	-2.717885000	17.026147000	17.754944000

Table S19. Cartesian coordinates for the DFT-optimized structure of **[Co^{I}(*bapbpy*$^{\bullet-}$)Cl)]$^{-}$** (**[1-Cl]$^{-}$**)

27	-5.253849000	13.156137000	15.924133000
17	-7.634959000	13.452185000	16.391359000
7	-3.520365000	13.073587000	17.047495000
7	-4.623642000	15.101556000	15.831477000
7	-3.344345000	10.715739000	17.189346000
1	-2.755139000	9.996497000	17.581066000
7	-5.352677000	13.280970000	13.791405000
6	-3.078869000	14.352421000	17.454359000
7	-5.929699000	15.582500000	13.958692000
1	-6.374035000	16.337680000	13.458261000
6	-3.669593000	15.446188000	16.782931000
6	-1.512695000	13.336864000	19.003375000
1	-0.743016000	13.421288000	19.765137000
6	-4.593565000	8.807154000	16.501663000
1	-3.796516000	8.180679000	16.892955000
6	-2.955653000	12.004976000	17.610741000
6	-6.312163000	13.263623000	11.149563000
6	-1.949882000	12.057473000	18.578470000
1	-1.537018000	11.146898000	19.000858000
6	-2.072144000	14.461774000	18.452120000
1	-1.739621000	15.444189000	18.768740000
6	-5.871627000	14.404199000	13.239568000
7	-5.434819000	11.029988000	16.095776000
6	-6.370416000	14.414467000	11.921967000
1	-6.786080000	15.333352000	11.518781000
6	-4.476714000	10.213801000	16.583600000
6	-5.086475000	16.024249000	14.999350000
6	-5.263510000	12.187274000	13.001116000
1	-4.812172000	11.321214000	13.471940000
6	-6.731366000	9.093064000	15.463353000
1	-7.645494000	8.704632000	15.028890000
6	-6.542975000	10.458189000	15.571375000
1	-7.302328000	11.172667000	15.268310000
6	-5.719294000	8.245653000	15.931433000
1	-5.817284000	7.165967000	15.867234000
6	-5.723204000	12.122520000	11.696723000
1	-5.633633000	11.199770000	11.134023000
1	-6.699969000	13.264459000	10.135560000
6	-3.924614000	17.772273000	16.156668000
6	-3.360518000	16.826395000	16.975285000
6	-4.784598000	17.381720000	15.097650000
1	-3.692524000	18.824206000	16.299825000
1	-5.180528000	18.101053000	14.388662000
1	-2.682985000	17.126827000	17.766680000

Table S20. Cartesian coordinates for the DFT-optimized structure of **[Co^{I}(*bapbpy*$^{-}$)]^{0}** (**[1]^{0}**)

27	-4.808534000	13.000724000	15.645418000
7	-3.345004000	13.018168000	17.031471000
7	-4.539409000	14.976971000	15.767664000
7	-3.283172000	10.679289000	17.271871000
1	-2.799174000	9.944692000	17.767978000
7	-5.266560000	13.258836000	13.574953000
6	-2.963690000	14.299321000	17.422880000
7	-5.955100000	15.501077000	13.959556000
1	-6.436385000	16.274588000	13.523340000
6	-3.634280000	15.364404000	16.759031000
6	-1.409205000	13.328553000	18.999190000
1	-0.640005000	13.437069000	19.757121000
6	-4.771473000	8.873721000	16.835152000
1	-4.120586000	8.245988000	17.436225000
6	-2.828873000	11.956057000	17.641558000
6	-6.392211000	13.372968000	11.020610000
6	-1.844985000	12.039782000	18.631170000
1	-1.451326000	11.149825000	19.109206000
6	-1.962531000	14.445445000	18.415528000
1	-1.624714000	15.432856000	18.705911000
6	-5.877847000	14.385299000	13.150745000
7	-5.221191000	11.059707000	15.910246000
6	-6.470195000	14.456378000	11.869069000
1	-6.961816000	15.372097000	11.555865000
6	-4.443866000	10.234072000	16.662878000
6	-5.116853000	15.918100000	15.020046000
6	-5.183137000	12.220307000	12.716084000
1	-4.658484000	11.352538000	13.101302000
6	-6.729415000	9.203230000	15.505197000
1	-7.641323000	8.851162000	15.037748000
6	-6.351010000	10.519242000	15.371250000
1	-6.955854000	11.210916000	14.795683000
6	-5.907394000	8.349507000	16.253195000
1	-6.160967000	7.304017000	16.389421000
6	-5.716840000	12.222476000	11.442806000
1	-5.615203000	11.353592000	10.803944000
1	-6.835722000	13.424642000	10.031564000
6	-4.113608000	17.687900000	16.287332000
6	-3.453920000	16.742933000	17.035404000
6	-4.954532000	17.284503000	15.226079000
1	-3.977699000	18.743971000	16.495681000
1	-5.435069000	18.009032000	14.577926000
1	-2.798451000	17.050178000	17.841260000

Table S21. Cartesian coordinates for the DFT-optimized structure of **[Co^{I}(*bapbpy*$^{\bullet-}$)(C**OO**)]** (**[1-(C**OO**)]**^{0})

27	-5.157942000	13.049283000	15.887712000
7	-3.514638000	13.023820000	17.095872000
7	-4.677378000	15.022131000	15.869588000
7	-3.406035000	10.670550000	17.280881000
1	-2.852368000	9.938672000	17.702530000
7	-5.435724000	13.278306000	13.765646000
6	-3.105923000	14.292700000	17.494357000
7	-6.037514000	15.558193000	14.031997000
1	-6.512180000	16.324310000	13.576897000
6	-3.764233000	15.381503000	16.848272000
6	-1.519709000	13.298986000	19.019434000
1	-0.734870000	13.392717000	19.762637000
6	-4.768484000	8.796722000	16.735660000
1	-4.023318000	8.160550000	17.202657000
6	-2.973191000	11.951189000	17.671582000
6	-6.453062000	13.332372000	11.168204000
6	-1.965215000	12.019650000	18.632533000
1	-1.555804000	11.119965000	19.077845000
6	-2.085011000	14.423115000	18.465377000
1	-1.742833000	15.406148000	18.763864000
6	-5.984649000	14.407676000	13.275745000
7	-5.462831000	11.016649000	16.117210000
6	-6.528804000	14.447944000	11.972091000
1	-6.984466000	15.363914000	11.609903000
6	-4.564221000	10.196172000	16.702364000
6	-5.221571000	15.967161000	15.103474000
6	-5.348162000	12.208886000	12.949957000
1	-4.875262000	11.335618000	13.386349000
6	-6.859274000	9.112152000	15.616347000
1	-7.782032000	8.737994000	15.190403000
6	-6.591719000	10.463833000	15.608175000
1	-7.294918000	11.176108000	15.192701000
6	-5.910489000	8.257232000	16.189025000
1	-6.072706000	7.184820000	16.218035000
6	-5.827468000	12.179831000	11.655866000
1	-5.728360000	11.285347000	11.053212000
1	-6.861739000	13.358489000	10.163281000
6	-4.176924000	17.711173000	16.369584000
6	-3.545879000	16.751794000	17.126709000
6	-5.014183000	17.328897000	15.301990000
1	-4.015506000	18.763775000	16.576801000
1	-5.463386000	18.063959000	14.643626000
1	-2.889638000	17.044148000	17.936865000
6	-6.837024000	13.564468000	16.978661000
8	-6.726936000	13.811945000	18.144564000
8	-7.574946000	13.405589000	16.021426000

Table S22. Cartesian coordinates for the DFT-optimized structure of **[Co^{I}(*bapbpy*$^{\bullet-}$)(OCO)] ([1-(O**CO)]^{0}**)**

27	-5.142673000	13.130048000	15.974701000
7	-3.442818000	13.063897000	17.104073000
7	-4.581887000	15.079562000	15.909556000
7	-3.359176000	10.703239000	17.372970000
1	-2.854492000	9.984861000	17.871750000
7	-5.456503000	13.340998000	13.846626000
6	-2.946560000	14.315406000	17.441281000
7	-6.096443000	15.599839000	14.195044000
1	-6.608342000	16.362631000	13.775200000
6	-3.588920000	15.430469000	16.788056000
6	-1.294457000	13.322647000	18.881828000
1	-0.460455000	13.409106000	19.569572000
6	-4.848428000	8.871585000	17.053094000
1	-4.193791000	8.268865000	17.674125000
6	-2.879988000	11.979836000	17.670426000
6	-6.537716000	13.434736000	11.278256000
6	-1.800892000	12.061341000	18.550304000
1	-1.372593000	11.159454000	18.974510000
6	-1.871580000	14.449888000	18.333197000
1	-1.491373000	15.432148000	18.582665000
6	-6.044178000	14.466640000	13.397771000
7	-5.311046000	11.003643000	16.041015000
6	-6.621109000	14.529871000	12.113871000
1	-7.106137000	15.443548000	11.786113000
6	-4.536428000	10.222588000	16.809027000
6	-5.172887000	16.020456000	15.165961000
6	-5.348263000	12.298030000	12.998900000
1	-4.834188000	11.432614000	13.401124000
6	-6.823428000	9.143518000	15.726571000
1	-7.741328000	8.771755000	15.288203000
6	-6.453160000	10.466740000	15.537700000
1	-7.045328000	11.121669000	14.916050000
6	-5.997815000	8.332132000	16.497040000
1	-6.249238000	7.291566000	16.674077000
6	-5.863281000	12.292401000	11.717257000
1	-5.753037000	11.418184000	11.087301000
1	-6.974977000	13.474114000	10.286087000
6	-3.951067000	17.753825000	16.276627000
6	-3.275260000	16.788336000	16.993539000
6	-4.906184000	17.376628000	15.318539000
1	-3.729007000	18.804214000	16.431164000
1	-5.406493000	18.115242000	14.702152000
1	-2.519066000	17.075807000	17.712675000
6	-8.046462000	12.586607000	16.706050000
8	-7.062930000	13.375293000	16.649722000
8	-9.207004000	12.671025000	17.018753000

Table S23. Crystal data and structure refinement for **[2-Cl_2]^0**.

Empirical formula	C20 H16 Cl2 Co N6
Formula weight	470.22
Temperature	150(2) K
Wavelength	0.71073 A
Crystal system	Monoclinic
Space group	P 21/c
Unit cell dimensions	a = 15.4767(3) A alpha = 90 deg.
	b = 14.4574(2) A beta = 100.3316(15) deg.
	c = 8.89585(14) A gamma = 90 deg.
Volume, Z	1958.20(6) A^3, 4
Density (calculated)	1.595 g/cm^3
Absorption coefficient	1.169 mm^{-1}
F(000)	956
Crystal size	0.243 x 0.138 x 0.129 mm
Theta range for data collection	1.942 to 30.507 deg.
Limiting indices	-22<=h<=21, -20<=k<=20, -12<=l<=12
Reflections collected	23481
Independent reflections	5983 [R(int) = 0.0289]
Absorption correction	Analytical
Max. and min. transmission	0.996 and 0.994
Refinement method	Full-matrix least-squares on F^2
Data / restraints / parameters	5983 / 0 / 326
Goodness-of-fit on F^2	1.031
Final R indices [I>2sigma(I)]	R1 = 0.0310, wR2 = 0.0660
R indices (all data)	R1 = 0.0418, wR2 = 0.0697
Extinction coefficient	n/a
Largest diff. peak and hole	0.393 and -0.333 $e.A^{-3}$

Table 24. Crystal data and structure refinement for **[1-Cl]**$^{+}$.

Empirical formula	C20 H16 Cl2 Co N6
Formula weight	470.22
Temperature	150(2) K
Wavelength	0.71073 A
Crystal system	Monoclinic
Space group	I 2/a
Unit cell dimensions	a = 13.3526(14) A alpha = 90 deg.
	b = 18.7885(15) A beta = 110.170(12) deg.
	c = 16.0864(17) A gamma = 90 deg.
Volume, Z	3788.2(7) A^3, 8
Density (calculated)	1.649 g/cm^3
Absorption coefficient	1.209 mm^{-1}
F(000)	1912
Crystal size	0.426 x 0.235 x 0.079 mm
Theta range for data collection	1.953 to 30.505 deg.
Limiting indices	-19<=h<=9, -7<=k<=26, -21<=l<=22
Reflections collected	11661
Independent reflections	5742 [R(int) = 0.0469]
Absorption correction	Analytical
Max. and min. transmission	0.978 and 0.924
Refinement method	Full-matrix least-squares on F^2
Data / restraints / parameters	5742 / 0 / 262
Goodness-of-fit on F^2	1.126
Final R indices [I>2sigma(I)]	R1 = 0.0635, wR2 = 0.1278
R indices (all data)	R1 = 0.0919, wR2 = 0.1418
Extinction coefficient	n/a
Largest diff. peak and hole	1.441 and -0.579 $e.A^{-3}$

References

1. Neese, F. Wiley Interdiscip. Rev. Comput. Mol. Sci. 2012, 2, 73.
2. Perdew, J. P. Phys. Rev. B 1986, 33, 8822.
3. Perdew, J. P. Phys. Rev. B 1986, 34, 7406.
4. Becke, A. D. Phys. Rev. A 1988, 38, 3098.
5. Schäfer, A.; Huber, C.; Ahlrichs, R. J. Chem. Phys. 1994, 100, 5829.
6. Neese, F. J. Comput. Chem. 2003, 24, 1740.
7. Weigend, F. PhysChemChemPhys 2006, 8, 1057.
8. Klamt, A.; Schürmann, G. J. Chem. Soc., Perkin Trans. 2 1993, 799.
9. Becke, A. D. J. Chem. Phys. 1993, 98, 1372.
10. Lee, C. T.; Yang, W. T.; Parr, R. G. Phys. Rev. B 1988, 37, 785.
11. L. Noodleman, *J. Chem. Phys.* **1981,** *74*, 5737.
12. L. Noodleman, D. A. Case, *Adv. Inorg. Chem.* **1992,** *38*, 423.
13. L. Noodleman, E. R. Davidson, *Chem. Phys.* **1986,** *109*, 131.
14. Yanai, T.; Tew, D.; Handy N., *Chem. Phys. Lett.*, **2004**, *393*, 51-57.
15. Casida, M. E., In *Recent Advances in Density Functional Methods*, Chong, D.P. Ed. World Scientific: Singapore, **1995**.
16. Stratmann, R. E.; Scuseria, G. E.; Frisch, M. J., *J. Chem. Phys.* **1998,** *109*, 8218-8224.
17. Bauernschmitt, R.; Ahlrichs, R., *Chem. Phys. Lett.* **1996**, 454-464.
18. Hirata, S.; Head-Gordon, M., *Chem. Phys. Lett.* **1999,** *314*, 291-299.
19, Hirata, S.; Head-Gordon, M., *Chem. Phys. Lett.* **1999,** *302*, 375-382.
20. Neese, F. *J. Chem. Phys*. 2001, 115, 11080.
21. Chemcraft, Chemcraft, http://chemcraftprog.com